Journal of the Korean Physical Society, Vol. 64, No. 12, June 2014, pp. L1783∼L1787 Letters

Resonant Production of Sbottom via RPV Couplings at the LHeC

S. Kuday*

Institute of Accelerator Technologies, Ankara University, Ankara, Turkey and Istanbul Aydin University, Department of Electrical-Electronics Engineering, Sefakoy, Kucukcekmece, 34295, Istanbul, Turkey

(Received 10 March 2014, in final form 23 April 2014)

Resonant production of scalar bottom, which is allowed in R-parity violating interactions of supersymmetry, has been investigated at the Large Hadron Electron Collider (LHeC). Although searching for the physics beyond the standard model is a primary task of the Large Hadron Collider (LHC) program, recently, an $e^- p$ collider (LHeC) was proposed to complement and resolve the observation of new phenomena at the TeV scale. In this paper, we address the prospects of improving constraints for $\hat{L}\hat{Q}\hat{D}$ couplings λ'_{ijk} through the process $e^- + p \to \widetilde{b}^* \to \mu^- + \overline{q}$, where q denotes up-type quarks. We show that constraints on λ'_{ijk} can be improved up to 10^{-3} for a 1 fb^{-1} integrated luminosity at a confidence level 95% with the 60 GeV e^- beam option of the LHeC.

PACS numbers: 14.80.Ly, 11.30.Pb, 12.60.Jv
Keywords: R-Parity, Violating, Supersymmetry, Sbottom, LHeC, Couplings
DOI: 10.3938/jkps.64.1783

I. INTRODUCTION

The theoretical structure of supersymmetry (SUSY), which has recently been an active area of research and interest at the Large Hadron Collider (LHC), allows gauge-invariant and renormalizable interactions that violate the conservation of the lepton and the baryon numbers. In the framework of the minimal supersymmetric standard model (MSSM), these interactions are forbidden by imposing an additional global symmetry that leads to the conservation of a multiplicative quantum number R-parity [1], which is defined as $R = (-1)^{3(B-L)+2S}$, where B, L and S are the baryon number, the lepton number and the spin, respectively. As a natural consequence of this phenomenology, all the SM particles and the Higgs boson have even R-parity ($R = +1$) while all the sfermions, gauginos and higgsinos have odd R-parity ($R = -1$). One of the highest motivations for the R-parity conserved MSSM is that it provides for sparticles to be produced in pairs because two odd particles always give an even number of R-parity. Although no SUSY signal has been detected yet, pair production of sparticles may be an important clue for the final states in SUSY searches at the LHC.

From the theoretical grounds for the SUSY, one could infer that R-parity conservation is actually inherited from conservations of the B and the L quantum numbers, which are natural consequences of a renormalizable and a Lorentz invariant theory. For such an extended SM theory, it is not necessary to keep those variables that are still conserved as long as the algebraic structure is safe. Although non-conservations of both the B and the L quantum numbers lead to rapid proton decay, a firm restriction to RPV (R-Parity violation) couplings guarantees a stable proton. Furthermore, allowing many of the interactions with the sparticles in the RPV SUSY model provides even richer phenomenology compared to the other models. However, many of the interactions in these terms may appear to be strictly supressed in nature. Thus, practical application of R-Parity violation in the MSSM also reveals several implications: firstly, sparticles can be produced in resonance processes, as well as in pairs, and secondly stabilization of particles (*e.g.*: dark matter) may not be guaranteed directly. In the context of the bilinear RPV model both the gravitino [2, 3] and the axino [4] as dark matter have been shown to be consistent with a lifetime exceeding the age of the universe. If the neutrino issue in the SM is considered, bilinear R-Parity violation which is induced by bilinear terms in the superpotential, can explain the neutrino masses and mixings in a way that is compatible with the current data without invoking any Grand Unified Theory (GUT) scale physics [5].

From the recent experimental data, the highest constraints for the gluino mass have reached about 1.5 TeV with 95% C.L. in Gauge-Mediated Supersymmetry Breaking (GMSB) and Constrained-MSSM (CMSSM) searches at $\sqrt{s} = 8\,TeV$ according to the A Toroidal LHC Apparatus (ATLAS) [6] and the Compact Muon

*E-mail: kuday@science.ankara.edu.tr; kuday@cern.ch; sinankuday@aydin.edu.tr

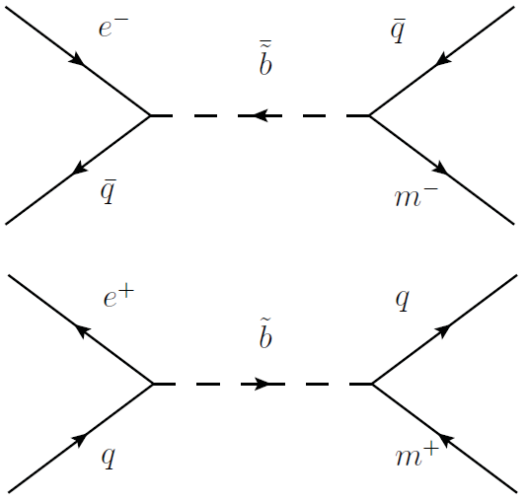

Fig. 1. Feynman diagrams of signal production where $q = u, c$ quarks.

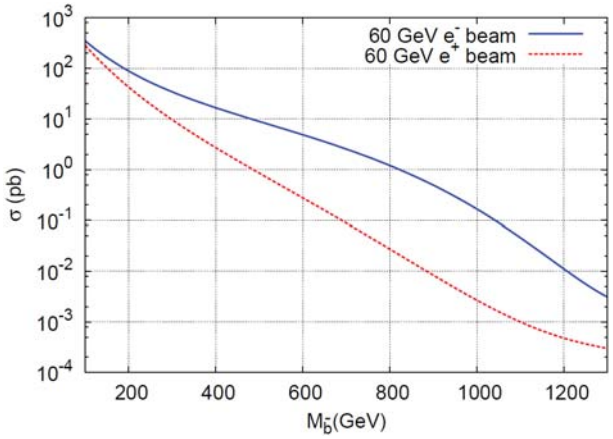

Fig. 2. (Color online) Cross sections vs. sbottom mass.

Solenoid (CMS) [7] results. For the stop and the sbottom masses, recent constraints are $m(\tilde{t}) > 660GeV$ [8] for $L = 20.5\, fb^{-1}$ and $m(\tilde{b}) > 620\, GeV$ [9] for $L = 12.8\, fb^{-1}$ at the LHC. Ongoing research that can be interpreted in the context of R-parity-violating supersymmetric scenarios at the LHC have set the limits $\tilde{q} > 1\, TeV$ [10,11] for squark masses and for RPV couplings λ'_{113} and λ'_{231} [12].

As a continuation of the LHC physics program, the Large Hadron Electron Collider (LHeC) [13,14] can extend research into the unexplored high-mass regions by using the linac-ring configuration implemented in the concept design report (CDR) [15] to continue technical design work. We should emphasize that the parameter space that will be covered at the LHeC also intersects with the LHC searches so that the main motivation of this work will be to compare limits between the LHeC as the future collider and the LHC as the present collider and to search for a possibility to improve those limits. After the LHeC starts running at full power, the first task will be to reconsider those limits and to improve them to constrain R-parity-violating squarks. Throughout this work, we will consider the basic energy options as the main reference for the LHeC, namely, $e^{\pm} = 60$ GeV and $p = 7$ TeV with $L = 10^{33}\, cm^{-2}s^{-1}$.

II. SIGNAL PRODUCTION AND DECAY VIA RPV INTERACTIONS

The R-parity-violating extension of the MSSM superpotential is given by

$$W_{RPV} = \frac{1}{2}\lambda_{ijk}\epsilon^{ab}L_i^a L_j^b \overline{E}_k + \lambda'_{ijk}\epsilon^{ab}L_i^a Q_j^b \overline{D}_k + \frac{1}{2}\lambda''_{ijk}\epsilon^{\alpha\beta\gamma}\overline{U}_i^{\alpha}\overline{D}_j^{\beta}\overline{D}_k^{\gamma} \quad (1)$$

where $i, j, k = 1, 2, 3, 4$ are the family indices $a, b = 1, 2$ are the $SU(2)_L$ indices and α, β, γ are the $SU(3)_C$ indices. $L_i(Q_i)$ are lepton (quark) $SU(2)$ doublet superfields; $E_i(D_i, U_i)$ are the charged lepton (down-type and up-type quark) $SU(2)$ singlet superfields. The couplings λ_{ijk} and λ''_{ijk} correspond to the lepton-number-violating and the baryon-number-violating couplings, respectively. One can easily see that the λ'_{ijk} coupling constants are antisymmetric under the exchange of the first two indices, and the λ'_{ijk} part of the Lagrangian can be extracted as

$$L_{\lambda'} = -\lambda'_{ijk}[d^{\dagger}_{Rk}\overline{\nu^c_i}P_L d_j + \tilde{d_{Lj}}\bar{d}_k P_L \nu_i + \tilde{\nu}_i d_k P_L d_j - d^{\tilde{\dagger}}_{Rk}\bar{e^c_i}P_L u_j - \tilde{e_{Li}}\bar{d}_k P_L u_j - \tilde{u_{Lj}}\bar{d}_k P_L e_i] + h.c. \quad (2)$$

Here, the fourth term directly corresponds to the vertex factors of the diagrams in Fig.1. Those, one can write the parton-level differential cross section for the signal in the rest frame of final muon and quark states as

$$\frac{d\sigma}{d\Omega} = \frac{(\lambda'_{123}\lambda'_{232})^2}{(16\pi)^2}\frac{\hat{s}}{\widehat{(\hat{s} - m^2_{\tilde{b}})^2} - (\Gamma m_{\tilde{b}})^2} \quad (3)$$

where $m_{\tilde{b}}$ is the sbottom mass and Γ is the total width of the sbottom, which can be calculated as $(\lambda'_{ijk})^2 m_{\tilde{b}}/8\pi$.

Because we take the single dominance hypothesis for granted, the lighter sbottom mass eigenstate will be the actual object here whenever we refer to the sbottom. For the signal production, one could immediately calculate that the contributions of other down-type scalar superpartners are negligible and that the parton-level contributions of all other quarks are minor except for those of u and c quarks. Therefore, we have taken into account these contributions to evaluate the total cross sections, as shown in Fig.2 by using the COMPHEP [16] event generator and the CTEQ6M PDF [17] package. In SUSY phenomenology, the magnitudes of the RPV couplings are arbitrary, so they are restricted only by phenomenological considerations. Therefore, two standard bounds are taken as [18]

$$\lambda'_{113} = \lambda'_{123} \leq 0.18\,, \qquad \lambda'_{231} = \lambda'_{232} \leq 0.45 \quad (4)$$

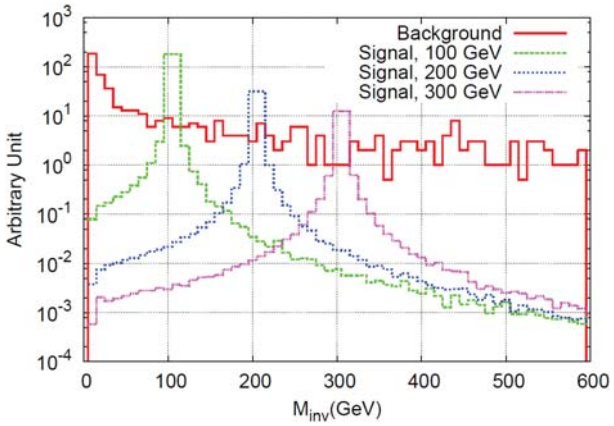

Fig. 3. (Color online) Invariant mass distributions of the signal and the background.

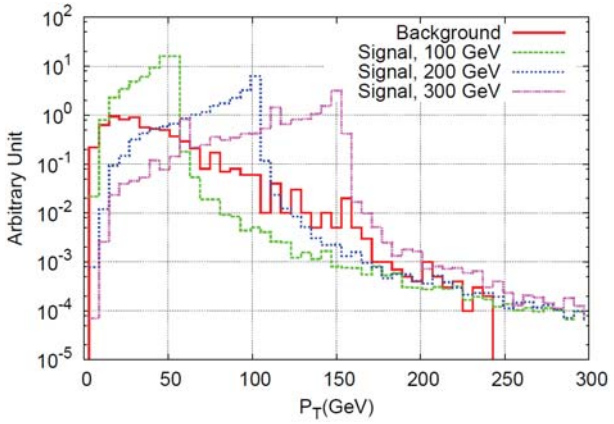

Fig. 4. (Color online) Transverse momenta for jets.

Here, it is worthwhile to emphasize that for the electron and the positron beam options, calculations explicitly show that the e^--beam options always deliver the highest cross section values, even for the 60 GeV e^--beam option in the low-mass region. This result seems to be contrary to the stop resonance production at the LHeC [19] where the e^+-beam option delivers higher cross section values. The main reason for the difference is related to the subprocess $e^- + q \to \widetilde{b}^* \to \mu^- + \overline{q}$, where q denotes u and c quarks whereas for stop production, the main contribution comes from b quarks in the initial state. Therefore, the equation [3] yields to signal values stronger than that of the stop resonance production. For the rest of this work, we choose the 60 GeV e^--beam option as the default option for investigating kinematical distributions and exclusion limits.

III. BACKGROUND PROCESSES

The process $e^\pm + p \to \mu^\pm + q/\bar{q} + X$, where q denotes u and c quarks seems to be the main background

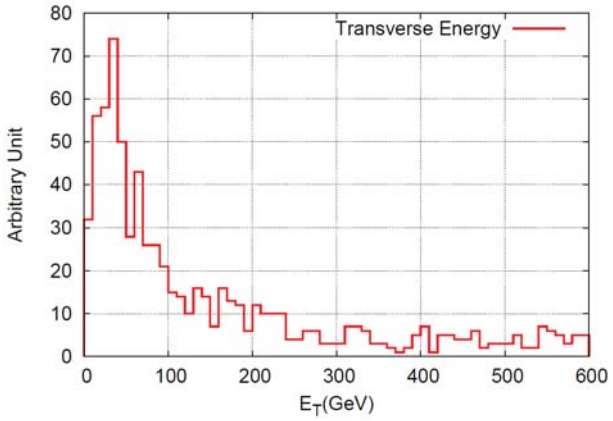

Fig. 5. (Color online) Missing transverse energy of the total background.

source for both beam options at the LHeC. The reducible SM background comes through the subprocess $e^- + p \to \nu_e + q/\bar{q} + W^-$, where the W boson rapidly decays via $\mu^-\bar{\nu}_\mu$ channel. Note that vetoing the contributions of $b/\bar{b}$ quarks in the final state reduces these subprocesses by a considerable amount. In an experimental point of view, the background may be reduced even more if the c-tagging option is implemented for the final-state quarks. In our case, we did not take into account any c-tagging options because of the very low tagging efficiencies. We obtained the comparisons of the kinematic distributions for the backgrounds and for the RPV signals by using PYTHIA 6.4 [20] and COMPHEP [16] software respectively, as shown in Fig. 3 and 4. We have built a new model implementing RPV interactions and vertex factors in the COMPHEP package for the signal while we have used the SM event generator PYTHIA 6.4 [20] for the background with normalization over 10^4 events. The P_T (transverse momenta) distributions of the jets in the final states will be naturally on the order of the half sbottom mass because outgoing particles, muon and jets are back-to-back in the transverse plane, neglecting the missing transverse energy. Also because we have neutrinos that will escape from detection in the final states with a significant missing transverse energy, having a non-zero $\not{E}_T$ distribution as in Fig.5 is important.

IV. EVENT SELECTION AND DISCUSSION

For the event selection part of the analysis, a strict strategy was previously introduced for RPV resonance particles [19] in order to reduce the large SM background. In our case, we developed the following cuts and optimizations:

- Kinematic cuts: for muons, $p_T^\mu > 25$ GeV and $|\eta_\mu| < 2.5$; for jets $p_T^q > 25$ GeV and $|\eta_q| < 3.5$.

Table 1. Required luminosities and cross sections of sbottom for the 60-GeV $e^{\pm}$ beam option of the LHeC at the 95% C.L. with $\lambda'_{113} = \lambda'_{123} = 0.18$ and $\lambda'_{231} = \lambda'_{232} = 0.45$.

$M_{\tilde{b}}$ (GeV)	$\sigma(e^-p)$ (pb)	Required $L_{int}(e^-p)(pb^{-1})$	$\sigma(e^+p)$ (pb)	Required $L_{int}(e^+p)(pb^{-1})$
100	211.78	0.022	201.38	0.023
200	38.39	0.154	22.17	0.318
300	13.71	0.492	4.85	2.5
400	6.82	1.192	1.35	18.836
500	3.76	2.683	0.41	157.761
600	2.1	5.707	0.13	1.382×10^3
700	1.11	13.547	3.78×10^{-2}	1.321×10^4
800	0.53	32.010	1.3×10^{-2}	7.3×10^4
900	0.21	79.491	2.1×10^{-3}	11.738×10^5
1000	6.55×10^{-2}	217.423	3×10^{-4}	14.37×10^6

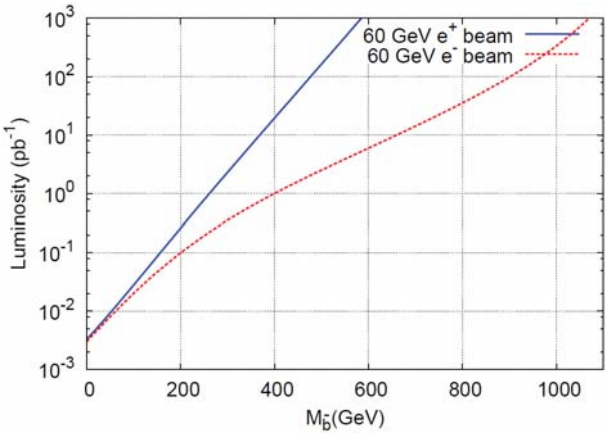

Fig. 6. (Color online) Integrated luminosity vs. sbottom mass for 95% C.L.

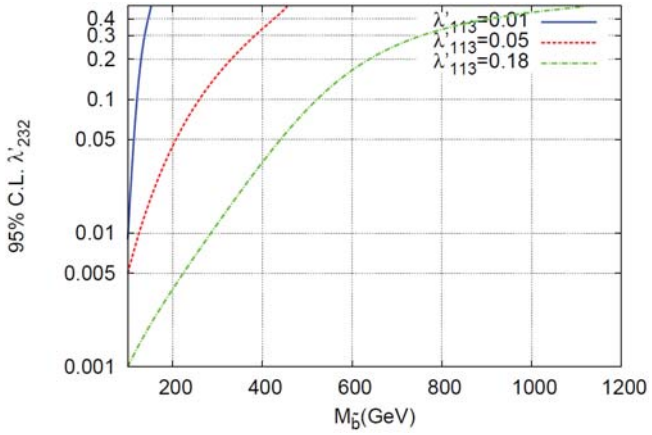

Fig. 7. (Color online) Attainable limits for the sbottom mass and RPV couplings at 60 GeV e^- beam option of LHeC.

- Missing transverse energy veto: $\not{E}_T < 25$ GeV.
- Invariant mass cut: $M_{\mu q} > 85$ GeV, and mass window cut in accordance with the energy resolution.
- Vetoing b-jets with 60% efficiency: Same assumption for b-jet identification in experiments because we need to identify b-jets before vetoing.

After the above selection criteria had been implemented, background cross sections were calculated as 1.7 fb for 60 GeV e^--beam option and 1.6 fb for 60 GeV e^+-beam option. For signal production, events always survived at a rate not below than 85% for sbottom masses between 100 and 1000 GeV. In Table 1, one can see the required luminosities to reach the 2σ significance value (95% C.L.) for both the 60 GeV e^--beam and 60 GeV e^+-beam options. In the significance calculations, we have always used the $S/\sqrt{S+B}$ formulation where S is the number of signal events and B is the number of background events. Obviously, the LHeC can exclude sbottom mass up to 1000 GeV in its first runs with a 217.5 pb^{-1} integrated luminosity if there is no apparent excess from SM predictions of μ + jets final states. Likewise, we depicted an extended plot of Table 1 in Fig.6. Attainable limits for sbottom mass with respect to RPV couplings $\lambda'_{113} = \lambda'_{123}$ and $\lambda'_{231} = \lambda'_{232}$ are presented in Fig.7 at 60 GeV e^- beam option of LHeC for 1 fb^{-1} integrated luminosity. One can see here that the LHeC can exclude sbottom mass up to 1200 GeV. The main reason for the $\lambda'_{113} = 0.18$ line extending to the high-mass region is a few backgrounds events that survived after selection criteria. With respect to the recent limits of the sbottom mass ($\tilde{}$ 700 GeV), the minimum attainable limit on the RPV couplings λ'_{232} is calculated to be around 0.25 for a fixed value of $\lambda'_{113} = 0.18$.

V. CONCLUSION

In this study, we introduced a phenomenological approach for constraining $\hat{L}\hat{Q}\hat{D}$ couplings via the RPV $e^- + p \to \widetilde{b}^* \to \mu^- + \overline{q}$ process ($q = u, c$). Resonance production of sparticles via RPV processes is a great advantage for obtaining a stronger signal although the specific final states can broaden the total background just as in our case for the final states of μ + jets. We implemented a stricter event selection in the limits of experimental capabilities to optimize the sensitivity of the signal. Considering the 60 GeV $e^{\pm}$ beam options of LHeC, we presented the cross sections and required luminosites at the 95% C.L. for $\lambda'_{113} = \lambda'_{123} = 0.18$ and $\lambda'_{231} = \lambda'_{232} = 0.45$ as well as the limits for the sbottom mass with respect to RPV couplings. In conclusion, with the 60 GeV e^- beam option, the LHeC can extend the exclusion limits of $\hat{L}\hat{Q}\hat{D}$ couplings up to 10^{-3} for 1 fb^{-1} integrated luminosity at the 95% C.L.

ACKNOWLEDGMENTS

I would like to express my greatest gratitude to Saleh Sultansoy for his fruitful discussions and helpful comments. This work is partially supported by The Turkish Accelerator Center (TAC) Project, Turkish Atomic Energy Authority (TAEA) and T.R. Ministry of Development.

REFERENCES

[1] R. Barbier *et al.*, Phys. Rept. **420**, 1 (2005).
[2] M. Fukugita and T. Yanagida, Phys. Lett. B **174**, 45 (1986); arXiv: 0005214 [hep-ph].
[3] M. Hirsch, W. Porod and D. Restrepo, JHEP **0503**, 062 (2005); arXiv:0503059 [hep-ph].
[4] E. J. Chun and H. B. Kim, JHEP **0610**, 082 (2006); arXiv:0607076 [hep-ph].
[5] W. Buchmuller, L. Covi, K. Hamaguchi, A. Ibarra and T. Yanagida, JHEP **0703**, 037 (2007), arXiv: 0702184 [hep-ph].
[6] G. Aad *et al.* (ATLAS Collaboration), arxiv:1210.1314 [hep-ex].
[7] S. Chatrchyan *et al.* (CMS Collaboration), arXiv:1303. 2985 [hep-ex].
[8] ATLAS Collaboration, Report No [ATLAS-CONF-2013-024].
[9] ATLAS Collabration, Report No [ATLAS-CONF-2012-165].
[10] G. Aad *et al.* (ATLAS Collaboration), arxiv:1210.7451 [hep-ex].
[11] CMS Collaboration, Report No: CMS PAS SUS-13-003.
[12] G. Aad *et al.*, (ATLAS Collaboration), Phys. Lett. B **723**, 15 (2013).
[13] The LHeC web page, http://www.lhec.org.uk.
[14] CERN-ECFA-NuPECC Workshop on the LHeC, Chavannes, Switzerland, June 2012; see http://cern.ch/lhec.
[15] J. L. Abelleira Fernandez *et al.* [LHeC Study Group Collaboration], J. Phys. G **39**, 075001 (2012); arXiv:1206.2913 [physics.acc-ph].
[16] E. Boos *et al.*, Nucl. Instrum. Meth. A **534**, 250 (2004).
[17] J. Pumplin, D. R. Stump, J. Huston, H. L. Lai, P. Nadolsky and W. K. Tung, JHEP **0207**, 012 (2002).
[18] R. Barbier *et al.*, Phys. Rept. **420**, 1 (2005).
[19] W.Hong-Tang, Z. Ren-You, G. Lei, H. Liang, M. Wen-Gan, L. Xiao-Peng and W. Ting-Ting, JHEP **1107**, 003 (2011); arXiv:1107.4461 [hep-ph].
[20] T. Sjostrand, S.Mrenna, P. Skands, [PYTHIA 6.4 Physics and Manual], JHEP **0605**, 026 (2006).